# Investigation of Certification Considerations for Distributed Electric Propulsion (DEP) Aircraft

May 1, 2022

Year 1 Final Report

U.S. Department of Transportation
**Federal Aviation Administration**

**NOTICE**

This document is disseminated under the sponsorship of the U.S. Department of Transportation in the interest of information exchange. The U.S. Government assumes no liability for the contents or use thereof. The U.S. Government does not endorse products or manufacturers. Trade or manufacturers' names appear herein solely because they are considered essential to the objective of this report. The findings and conclusions in this report are those of the author(s) and do not necessarily represent the views of the funding agency. This document does not constitute FAA policy. Consult the FAA sponsoring organization listed on the Technical Documentation page as to its use.

This report is available at the Federal Aviation Administration William J. Hughes Technical Center's Full-Text Technical Reports page: actlibrary.tc.faa.gov in Adobe Acrobat portable document format (PDF).

**Form DOT F 1700.7** (8-72)     Reproduction of completed page authorized

| 1. Report No. DOT/FAA/TC-22/15 | 2. Government Accession No. | 3. Recipient's Catalog No. |
|---|---|---|

| 4. Title and Subtitle | 5. Report Date |
|---|---|
| Investigation of Certification Considerations for Distributed Electric Propulsion (DEP) Aircraft | May 1, 2022 |
| | 6. Performing Organization Code ANG-E272 |

| 7. Author(s) R. McKillip, Jr., D. Wachspress | 8. Performing Organization Report No. CDI Report 22-01 |
|---|---|

| 9. Performing Organization Name and Address Continuum Dynamics, Inc. 34 Lexington Ave. Ewing, NJ 08618 | 10. Work Unit No. (TRAIS) |
|---|---|
| | 11. Contract or Grant No. 692M15-20-T-00040 |

| 12. Sponsoring Agency Name and Address AIR-714 FAA Central Regional Office Kansas City, MO 64106 | 13. Type of Report and Period Covered Year 1 Final Report 9/9/2020-5/1/2022 |
|---|---|
| | 14. Sponsoring Agency Code AIR-714 |

15. Supplementary Notes

As the sponsor for this project, we wanted to inform policy on appropriate safety metrics for control power margins. Our new Part 23 rules and special conditions are Performance Based but do not have specific guidance in this area. At the same time, we ask applicants to consider control power margins and crew awareness in the Rule: 23.2300. How do we address showing of compliance to this rule in the "urban wind jungle" with swirling winds around skyscrapers and landing on rooftops with high tempo operations? We hope some new ideas from this research will help applicants and the FAA come to agreement on appropriate safety metrics.

16. Abstract

Efforts from the first year of a multi-year investigation examining the use of estimation of both remaining vehicle control power margins and external environmental disturbances for distributed electric propulsion (DEP) vehicles as a contributor for vehicle certification are described. This study combines simulation of DEP aircraft with experimental testing of representative models in the assessment of algorithms for determining remaining control power margins in real-time operation of these vehicles, to provide a metric for the capability of that vehicle to accommodate operational disturbances and avoid loss of control (LOC) events. The Comprehensive Hierarchical Aeromechanics Rotorcraft Model (CHARM) analysis for aerodynamic interaction effects on these configurations is being used to simulate and characterize vehicle response to disturbances and to applied control inputs throughout its flight envelope. The goal of the effort is to determine the viability of the methods for calculation of remaining control power margins, and to assess the utility of the methods in safety monitoring of DEP flight operations for both manned and unmanned vehicles. This first year of research has shown that application of algorithms for estimating remaining available vehicle control power, and local gust disturbance magnitudes, appear to provide a usable safety assessment for avoiding loss of control (LOC) events for eVTOL/DEP aircraft. A follow-on research project will expand the algorithm application for control equivalent gust estimation and extraction of local disturbance flows.

| 17. Key Words Remaining control power, distributed electric propulsion, eVTOL aircraft, loss of control sensing | 18. Distribution Statement This document is available to the U.S. public through the National Technical Information Service (NTIS), Springfield, Virginia 22161. This document is also available from the Federal Aviation Administration William J. Hughes Technical Center at actlibrary.tc.faa.gov. |
|---|---|

| 19. Security Classif. (of this report) Unclassified | 20. Security Classif. (of this page) Unclassified | 21. No. of Pages | 19. Security Classif. (of this report) Unclassified |
|---|---|---|---|

# Contents

# Figures

# Tables

**No table entries found.**

# Acronyms

| Acronym | Definition |
|---------|------------|
| CDI | Continuum Dynamics, Inc. |
| CETI | Control equivalence turbulence input |
| CHARM | Comprehensive Hierarchical Aeromechanics Rotorcraft Model |
| DEP | Distributed electric propulsion |
| eVTOL | Electric vertical takeoff and landing |
| FAA | Federal Aviation Administration |
| FlightCODE | Flight dynamics computation of ordinary differential equations |
| IMU | Inertial measurement unit |
| LOC | Loss of control |
| METAR | Meteorological aerodrome reports |
| METS | Mixer equivalent turbulence simulation |
| NASA | National Aeronautics and Space Administration |
| NDARC | NASA Design and Analysis of RotorCraft |
| PIREP | Pilot report |
| RCP | Remaining control power |
| SWaP | Size, weight and power |
| UAM | Urban air mobility |
| UAS | Unmanned aircraft system |
| UAV | Unmanned aircraft vehicle |
| UDB5 | UAV data board v5 |

# Executive summary

This report describes the first year of a multi-year effort examining the definition and algorithmic computation of remaining control power (RCP) as a metric for assessment of potential loss of control (LOC) events. Algorithms for computing RCP are being investigated through analysis, simulation, and testing on representative scaled vehicles having configurations that capture current design concepts in development within the distributed electric propulsion (DEP) vertical takeoff and landing (VTOL) space. These aircraft are characterized by multiple lifting rotors, that may articulate (along with attached wings) and/or are augmented by additional propulsion units and other lifting surfaces. Many DEP concepts provide redundant controls for safety enhancement, and all incorporate some form of feedback stabilization to aid flying qualities and provide disturbance rejection. Assessment of remaining control power, and its algorithmic computation, is challenged with this complexity, but to be successful, should be performed in as wide a context as possible for this class of vehicle. The guiding mission statement for this effort is in two parts:

- Investigate sensors and algorithms scalable to different vehicle sizes that compute control power margins for DEP VTOL aircraft accounting for the disturbance field and estimating local winds and gusts in real time.
- Use empirical data from algorithm use and lessons learned to suggest industry best practices and FAA policy for ensuring DEP VTOL vehicles operate safely without exceeding control power margins. Consider small unmanned aircraft system (UAS) as well as passenger carrying DEP VTOL vehicles.

The first year of this effort, described here, examined approaches for assessing RCP and disturbance response that required increasing levels of information on the vehicle flight control system, guidance commands, and in-flight responses. Several were demonstrated in limited degree-of-freedom simulations, and one was flight tested using a modified commercially available quadcopter. Those initial tests demonstrated the capability of the simplified algorithm to indicate potential LOC events through monitoring command inputs to flight control actuators. Continued research will expand both algorithm development and flight demonstrations to include vehicles with redundant control effectors and operations from vertical takeoff and landing to cruising flight.

# 1 Introduction

A major push in the development of urban air mobility (UAM) aircraft is underway that will potentially transform how we travel by providing on-demand, passenger-carrying operations in metropolitan areas. Dozens of organizations are currently in the process of developing air-vehicle concepts based on multi-prop (multi-propeller) aircraft using distributed electric propulsion (DEP) for potential use in future air-taxi services. New standards or combinations of existing ones may be necessary to certify airworthiness and safe design of these aircraft for their use in civil service. Developing a pathway to certification will require an in-depth understanding of the flight dynamics and control characteristics of complex, multi-prop, multicomponent aircraft flying new mission profiles in urban environments.

Recent modifications in Part 23 certification requirements have been implemented to change them from a prescriptive format to one that is performance-based. This change has allowed for rapid incorporation of advanced technologies onto flight vehicles that can promote safety that may not conveniently fit within the prescriptive certification basis structure as it existed. The research here is to identify techniques, algorithms, and methodologies that can provide onboard electric vertical takeoff and landing (eVTOL)/DEP safety assessment in real-time that would support this transition to performance-based certification standards.

This research program is conducting comprehensive modeling and analysis to achieve the following objectives:

1. Evaluate approaches for real time control power margin and wind monitoring including determining vehicle control states to be monitored and the impact of vehicle size, configuration, and degraded mode (e.g., thruster out) conditions.

2. Identify the most promising approaches and assess them within a representative vehicle using simulation modeling capability.

3. Demonstrate the concept using a sub-scale unmanned aircraft vehicle (UAV) in both controlled (laboratory or wind tunnel) and ambient conditions.

4. Evaluate implications for eVTOL and unmanned aircraft system (UAS) certification requirements.

# 2 Control power margins

Air vehicle controllability is fundamental to both safety and utility, as the aircraft controls must be capable of:

- trimming the vehicle in all phases of flight,

- providing added forces and moment for maneuvers, and

- compensating for disturbances encountered throughout the flight profile.

Unstable aircraft can be stabilized, through automatic or manual control, if the vehicle's controllability is of sufficient power (and responsiveness) to provide appropriate forces and moments to maintain flight operations. Much like conventional helicopters, eVTOL/DEP vehicles are intrinsically unstable in hover and require such control for rotor-borne flight operations. Therefore, feedback control for stabilization subtracts from the control power available for maneuvering and trim. However, these same aircraft, due to their placement of many motor-driven force generators around their vehicle exterior, often have redundant control capability (also called over-actuated aircraft) and thus can provide additional options for changes in flight vehicle states for executing certain maneuvers (e.g., separation of vehicle pitch attitude and velocity regulation, (McKillip & Perri, 1992)). These additional controls may also be leveraged to maintain trimmed flight in failure states, although potentially with reduced vehicle acceleration or maneuvering options. Thus, a useful metric for assessing remaining control power (RCP) on eVTOL/DEP aircraft must account for these impacts on the control system if it is to serve as an indicator of potential for loss of control (LOC) events.

Recent work (List & Hansman, 2019) directly addresses the use of control power ratios as metrics of vehicle controllability for multicopter eVTOL concepts. While that work generated those ratios using torque measurements on lift rotors, other control metrics may be needed for other configurations and flight modes. Fundamental to the use of remaining control power as a metric of potential for safety monitoring is the assumption that situations that lead to control saturation constitute LOC events. While such a characterization is generally true, there exist situations when maximum performance is being requested from a flight vehicle, and thus some controls may well be at their limit values – such as throttle settings on takeoff, for example. In addition, these limits on remaining control power can exist at several places within the control system itself. For pilot-controlled vehicles, stick/effector gearings may drive what vehicle control settings are possible, while physical installations of actuators and connected vehicle mechanics may have limits of their own on both displacements and actuation rates. Even the on-board control law may include limits of outputs to actuators to mitigate cases of potential hard-over commands or undesired runaway behavior, especially in limited-authority feedback systems. Thus, the mere approach of vehicle/system control limits alone are not themselves representative of safety margins – instead, it is the sum of the current control power *and the remaining control power required to compensate for vehicle response being other than that*

*commanded by the current control inputs* that define the safety margins. Figure 1 shows a conceptual picture of the contributions of ratioed trim inputs, maneuver commands, and disturbance rejection inputs on remaining available control power (shown shaded in green).
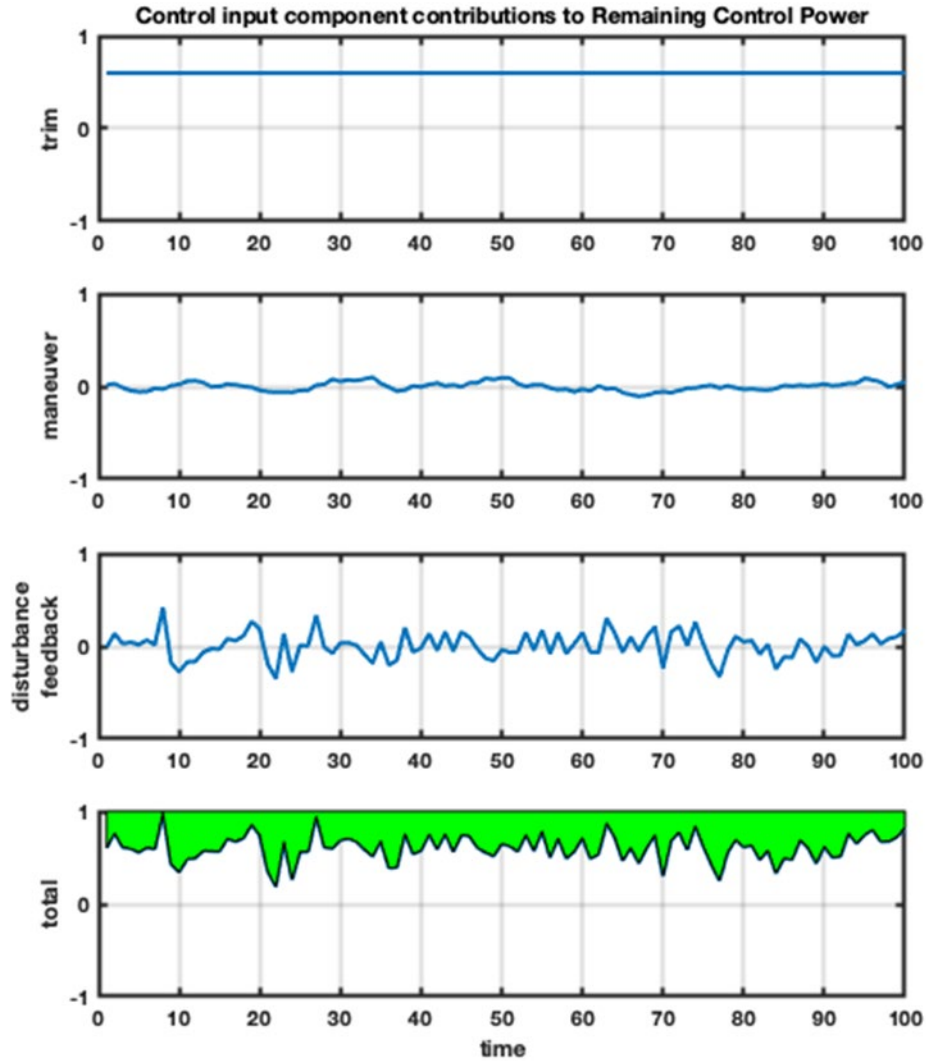


Figure 1. Contributions of control input sources to RCP

## 2.1   Control power metrics

Monitoring of all signals within the flight control system for possible limit exceedances to provide protection from LOC events would be impractical, particularly for any system of even moderate complexity.  With the premise that such a monitoring system should be as generic as possible across the range of eVTOL/DEP aircraft, the choice of control input that directly impacts the associated force/moment generator on the aircraft seems most appropriate.  For rotors/propellers, that would represent any control features available for changing thrust

magnitude or direction; for fixed-wing surfaces, control deflections of devices that change local camber or sectional shape should suffice.

While past monitoring of pilot effector displacements relative to physical limits has been effective for assessing potential LOC situations in flight test campaigns, the redundant control configurations found on proposed eVTOL/DEP aircraft, and the potential for fully autonomous (unpiloted) operation make this alternative more beneficial. An example of an autonomous octocopter having four displaced coaxial rotors and no pilot effectors serves to illustrate this scheme. Monitoring of each rotor's input command (rpm or collective) provides indication of its operating state and potential for thrust/torque magnitude changes and does not require measurement availability of guidance and control commands from the autopilot directing the vehicle's flight profile between takeoff and landing destinations. Also, in the event of a single motor failure and subsequent additional thrust generated from the companion unit on that coaxial rotor installation, the new command for the "working" rotor would directly indicate its operation at a state nearer maximum capability (reduced control power margin), as it would be generating approximately twice the thrust previously applied prior to the fault condition. This change, due to the fault accommodation of the feedback control system, would not be reflected in monitoring of the internal flight command signals within the navigation autopilot.

The eVTOL/DEP aircraft designs directly capitalize on the recent developments that have significantly boosted the power/weight ratios of electric motor drives, thus permitting their use in aviation applications. By distributing the sources of lift and propulsion, each rotor/propeller may be made smaller as it need not carry the full vehicle weight or drag load on its disk. And, by exploiting the convenience of individual electronic control, weight savings is realized through the elimination of mechanical cross-shafting between propulsors and lift systems. This same electronic control may also use direct motor speed control as a means of power/torque regulation at each rotor/propeller, potentially eliminating requirements for variable pitch control (collective and cyclic). However, this choice of control variable has some consequences.

Direct rpm or motor torque control, in the absence of rotor/propeller pitch adjustment, requires the blades to be accelerated or decelerated to the operating rpm needed for the desired level of thrust generation. Clearly, the size of the rotor will dictate the associated inertia and thus the resultant time constant for that rpm change, thereby controlling the available bandwidth in force modulation for that type of control (Withrow-Maser, Malpica, & Nagami, 2020). Conversely, direct pitch adjustment can provide an accelerating effect on force control, as a direct thrust change is first realized prior to the rotor/propeller wake adjusting to the new pitch change and thereby mitigating some of the initial effect from that perturbation in control.

Ratioing the current control input to a "prime mover" (force/moment generator) on a flight vehicle to its input range would give a fraction of control expenditure; subtracting that value from its limits gives a resulting ratio of remaining control power (authority) for that input. Thus, an easily computed metric for RCP on input *i* is shown in Equation 1.

$$RCP_i = min\left(2\frac{u_{max} - u_i}{u_{max} - u_{min}}, 2\frac{u_i - u_{min}}{u_{max} - u_{min}}\right) \qquad 1$$

This value generates a value of one when the control input is at the center of its range of travel, and zero when it reaches an upper or lower control limit bound. This metric has the distinct advantage that only the control limits available on the prime mover are necessary for its computation, as it is agnostic of vehicle type, configuration, or operating state. While those are desirable features, use of this metric for safety assessment assumes that the aircraft is in controlled flight as long as this value is below unity; and, this metric only has safety assessment value to the aircraft on which it is being computed. If considerations of vehicle response to this control are to be included in the safety assessment, via a different metric for remaining control power, or if any predictive capability is desired to assess needs for added control power, a model-based algorithm (of some order) must be used.

## 2.2 Model-based metrics

Monitoring control activity in real-time during flight operations using a model-based algorithm can have an additional benefit of providing estimates of disturbance effects as well, if one accepts that responses not due to control application occur solely from external flow fields (this assumes that controls on all force generators are nominal). Several researchers have developed algorithms for estimation of "wind states" that generate vehicle disturbances from comparisons between calibrated vehicle responses to control inputs and actual measured vehicle sensor data (McConville, Richardson, & Moradi, 2022; McKillip, Jr., 2018). Such estimates could potentially indicate turbulent environments within the current operational area that make continued flight too risky, or in need of revision (approach/departure directions, vehicle headings on takeoff and landing, etc.). Turbulent environment information could also be shared among other nearby aircraft, providing enhanced situational awareness and safety, much as wake turbulence warnings are often issued for local airport operations currently.

The relationship between control power and disturbance effects has been investigated by researchers at the National Aeronautics and Space Administration (NASA) Ames (e.g., (Lusardi, Blanken, & Tischler, 2003)) in the development of the concept of mixer equivalent turbulence

simulation (METS), or control equivalence turbulence input (CETI). The same concept and algorithm compute the residual between measured helicopter response and that predicted from measured control inputs, and then processes it through an inverse dynamic representation of the flight vehicle to estimate the equivalent amount of additional control needed to generate that differential (Seher-Weiss & von Gruenhagen, 2009). While the primary use of this representation was to permit simulation of turbulent effects in manned simulation trials, it is self-evident that if the combined (summed) control input levels approach limits on control capabilities of the flight vehicle, the potential for upset and loss of control is greatly increased. Although that would represent a direct relationship between disturbances present and required control to counter them, it requires use of an inverse dynamic model and thus is more vehicle-specific in its application versus the simpler technique described above.

# 3     Dual-estimator approach

The model-based approach adopted in the research here is effectively two-fold but has origins in the same basic concept – that of treating the vehicle *"holistically"* such that total vehicle response is either due to applied control from on-board effectors, or from external disturbances. This same concept has been used in the past at Continuum Dynamics, Inc. (CDI), most notably for icing accretion estimation based on measured performance metrics on an aircraft (McKillip, Keller, & Kaufman, 2002). The same estimator-based approach here is tasked with providing two metrics: the first represents the additional required control power to counter the disturbance measured on the flight vehicle, and the second is the magnitude and type of the external disturbance. The first of these is of direct interest for maintaining adequate control of the vehicle on its intended flight trajectory, while the second is of general interest to other aircraft operating in the vicinity of the present DEP vehicle computing that disturbance estimate. Thus, the remaining control power available directly impacts the present vehicle's level of safety, while the external gust disturbance estimate provides vehicle-context-fee information for sharing with other aircraft of different sizes and configurations, much like meteorological aerodrome reports (METAR) and pilot report (PIREP) information is provided to pilots at present.

## 3.1     Control-equivalent turbulence estimation

Generation of equivalent control power for mitigating a disturbance is effectively what is accomplished with the METS/CETI schemes described earlier, although here it is implemented in a real-time, time-domain context. A simple example looking at linearized (stability derivative) pitch-plane dynamics of an aircraft provides an example. Consider the linearized

response to both control input (primarily a moment command) and a longitudinal gust as shown in Equation 2.

$$\frac{d}{dt}\begin{Bmatrix} u \\ q \\ \theta \end{Bmatrix} = \begin{bmatrix} X_u & X_q & -g \\ M_u & M_q & 0 \\ 0 & 1 & 0 \end{bmatrix} \begin{Bmatrix} u \\ q \\ \theta \end{Bmatrix} + \begin{bmatrix} 0 \\ M_\delta \\ 0 \end{bmatrix} \{\delta_{lon}\} + \begin{bmatrix} X_u \\ M_u \\ 0 \end{bmatrix} \{u_{gust}\} \qquad 2$$

We can introduce an equivalent CETI gust "control" input in this same axis as shown in Equation 3.

$$\frac{d}{dt}\begin{Bmatrix} u \\ q \\ \theta \end{Bmatrix} = \begin{bmatrix} X_u & X_q & -g \\ M_u & M_q & 0 \\ 0 & 1 & 0 \end{bmatrix} \begin{Bmatrix} u \\ q \\ \theta \end{Bmatrix} + \begin{bmatrix} 0 \\ M_\delta \\ 0 \end{bmatrix} \{\delta_{lon}\} + \begin{bmatrix} 0 \\ M_\delta \\ 0 \end{bmatrix} \{\delta_{gust}\} \qquad 3$$

We can augment the state variables to treat this equivalent gust control as a random process as shown in Equation 4.

$$\frac{d}{dt}\begin{Bmatrix} u \\ q \\ \theta \\ \delta_{gust} \end{Bmatrix} = \begin{bmatrix} X_u & X_q & -g & 0 \\ M_u & M_q & 0 & M_\delta \\ 0 & 1 & 0 & 0 \\ 0 & 0 & 0 & 0 \end{bmatrix} \begin{Bmatrix} u \\ q \\ \theta \\ \delta_{gust} \end{Bmatrix} + \begin{bmatrix} 0 \\ M_\delta \\ 0 \\ 0 \end{bmatrix} \{\delta_{lon}\} + \begin{bmatrix} 0 \\ 0 \\ 0 \\ 1 \end{bmatrix} \{w_g\} \qquad 4$$

This formulation can be used in a recursive estimator, such as a Kalman Filter, to determine the unknown equivalent gust control input, and its variance (statistics), in real-time, on an aircraft, and it only requires a reasonable linearized dynamic model of its response. This time-domain formulation has several advantages:

1. Direct representation of gust "controls" within the dynamics equations avoids a requirement for conversion to frequency-domain parameterizations and inverting multiple transfer function expressions.

2. Gust control effects will excite all dynamic modes that can be affected by the available control components and can include all cross-couplings and interactions that may be present on a particular vehicle configuration.

3. Time-domain representation allows for tracking transient behavior and avoids inherent lags associated with representing signals in the frequency domain.

4. Model adjustment of control effectiveness can be applied for cases of reduced or inoperative control capability, with the gust control estimates adapting accordingly based on the updated dynamic model.

5. Steady-state filter estimator variance can be used to optimize the selection of vehicle sensors (resolution, noise floor, sampling rate, etc.) for determination of this equivalent control gust value.

6. On-line estimation of gust control variance provides added support in the determination of control limits that warrant remedial action or termination of flight activity.

7. And, choice of control for force/moment generation (individual components) or response command (vehicle force/moment aligned with an axis) can be accommodated in this simple model formulation.

This approach effectively maps the actual dynamic system response to a gust, to the system response to a control input, and thus in some sense gives an estimate of the *equivalent control that would have to be supplied to counter the disturbance of the gust on the aircraft*. A simple model for a quadcopter demonstrates that this technique provides a reasonable assessment of the equivalent control needed for generating a similar disturbance, as shown in Figure 2. This plot shows the actual response of the simulation model to a random gust, and that calculated from using the estimated equivalent control gust input to generate a control response. Apart from some high frequency tracking error, the estimated control gust magnitude provides a good estimate of how the vehicle responds to turbulence, and thus, is an appropriate metric on what ideal control would be needed to counter those effects. With this computed equivalent disturbance "control", the RCP metric from before is modified to use:

$$u_i = \delta_{control} + \delta_{gust} \qquad\qquad 5$$

(Equation 5) with the implication that if the disturbance effect cannot be accommodated with the current control and this ideal disturbance correction input, a control limit may occur and thus a potential LOC event, provoked by an excessive disturbance on the aircraft. Note that prediction of this control limit is not dependent upon any knowledge or assumptions concerning on-board feedback control functions, but just on a reduced-order model of the base, open-loop vehicle dynamics. An alternative use of the estimated disturbance "control" from the filtering process could include adding the estimation variance to this sum to provide even more protection from this stochastic disturbance "input."
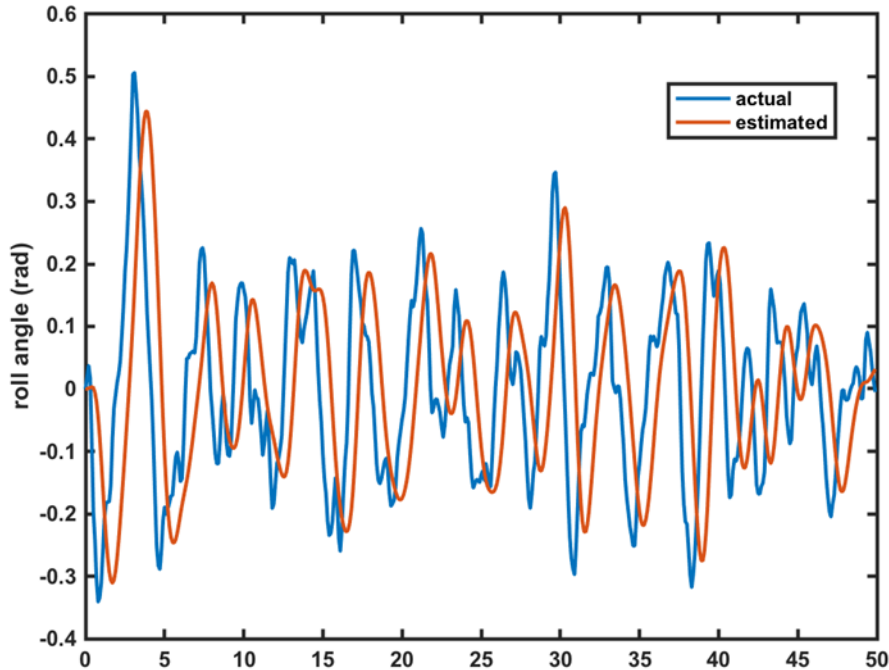
Figure 2. Simulated quadcopter response to gust and to control equivalent gust input

## 3.2 Recursive gust estimation

Knowledge of vehicle control activity relative to its limitations is certainly a viable indicator of the potential for a LOC event. However, the ability to directly sense or estimate the current environmental disturbance environment can provide an additional safety buffer on the amount of control power expected for maintaining adequate flight control and operational safety. Such information may be represented in the vehicle operator's manual or may be used in flight dispatch functions for enforcing limits on acceptable landing and departure operations.

Sensing of the turbulence environment using on-board systems can be done using discrete sensors or a holistic, performance-based method whereby models for full vehicle responses to turbulence are used to estimate what aerodynamic environment generated that response. In some sense, these two approaches are equivalent, except the holistic aircraft response approach requires the inversion of a higher-order dynamic model. Direct turbulence sensors include air data probes of appropriate bandwidth, autorotating propellers, or flow-angle vanes. Indirect vehicle measurements that show evidence of disturbances range from isolated accelerometers to full inertial measurement units (IMUs) with possible GPS-aided position and velocity data for a complete vehicle state estimation application (that can include gust disturbance states). Each approach has its benefits and disadvantages.

Discrete sensors typically represent a simpler approach for detection of flow states on an aircraft but must be placed in locations that do not have undue influence from local flow effects that arise from changes in secondary flows from operating state adjustments or interacting wake/wash effects. This interaction is why most flight test aircraft operate with long booms positioned forward of aircraft structure to sample flow conditions ahead of vehicle upwash and other flow gradients. A disadvantage of discrete sensor application is the requirement for extra hardware, power, and data transfer.

Similarly, complete holistic vehicle sensing must include all relevant effects in the system model if it is to unambiguously identify flow state changes from external disturbances, versus those from local trim changes or dynamic maneuvers. This separation is achieved through monitoring vehicle control commands and processing them with a dynamic model of the vehicle to generate an estimate of what the controlled response should be, to determine the measurement residual as due to external disturbances. Although this approach needs good measurement of control inputs, vehicle response, and a valid dynamic model, it does not carry a weight or volume requirement (size, weight, and power (SWaP) impact), as the sensing is performed algorithmically.

Direct turbulence field estimation can be viewed as a more global assessment of the vehicle disturbance environment than the control equivalent turbulence estimation approach described in the previous section. While knowledge of the control equivalent turbulence input to a specific aircraft is useful for assessment of potential loss of control from exceeding control power requirements on *that* vehicle, it is not generally transferrable information that has value to other disparate aircraft that may be operating in the same area. Direct estimation of gust velocities, however, can be generally shared among aircraft operating near one another (think of METAR reports on gusts), but still require aircraft-specific interpretation to gauge the severity of that measured disturbance.

Considering again a simplified linearized model for longitudinal response, and, noting that most of the significant impact of gusts on vehicle ride quality will affect the short period response, we can limit the states of interest to include just vertical velocity, pitch rate, and pitch attitude, and consequently, vertical gusts, giving the following dynamic system, where we have modeled the vertical gust as a first-order random process driven by white noise (Equation 6).

$$
\begin{bmatrix} \Delta\dot{w} \\ \Delta q \\ \Delta\dot{\theta} \\ \Delta\dot{w_g} \end{bmatrix} = \begin{bmatrix} Z_w & u_0 & -g\sin\theta_0 & -Z_w \\ M_w + M_{\dot{w}}Z_w & M_q + M_{\dot{w}}u_0 & 0 & -M_w - M_{\dot{w}}Z_w \\ 0 & 1 & 0 & 0 \\ 0 & 0 & 0 & -1/\tau \end{bmatrix} \begin{bmatrix} \Delta w \\ \Delta q \\ \Delta\theta \\ \Delta w_g \end{bmatrix} + \begin{bmatrix} Z_{\delta e} & Z_{\delta T} \\ M_{\delta e} + M_{\dot{w}}Z_{\delta e} & M_{\delta T} + M_{\dot{w}}Z_{\delta T} \\ 0 & 0 \\ 0 & 0 \end{bmatrix} \begin{bmatrix} \Delta\delta e \\ \Delta\delta T \end{bmatrix} + \begin{bmatrix} 0 \\ 0 \\ 0 \\ 1/\tau \end{bmatrix} [v2]
$$

6

This representation lends itself (again) directly to implementation of a Kalman Filter for estimating aircraft states along with noise values that automatically include variance estimates as part of the covariance calculation within the filter structure. This approach has several advantages which include:

1. Direct estimation of gust disturbance in real-time using aircraft instrumentation.

2. Simplified algorithmic processing that is low-order and thus easily hosted on available processors.

3. Computation of gust metrics that are not vehicle-specific and can be shared with nearby aircraft for their own safety assessment.

This simple representation, however, may not always capture the primary gust effects encountered by an eVTOL/DEP configuration, particularly if spatial distributions of the gust (gust gradients) are on the same length scale as the distances separating lift rotors. In those events, significant moment inputs would be expected on the vehicle other than those from a "uniform" gust value distributed across the airframe. Hence, it may be of interest to include equivalent pitch rate "gust" effects for this restricted longitudinal model as well, expanding the degrees of freedom that would be used to represent the turbulent environment surrounding the aircraft.

# 4    Simulation assessment

While the limited degree-of-freedom stability derivative models have suggested this dual estimation approach is a viable technique for online estimation of both remaining control power in the presence of disturbances and the gust disturbance magnitudes themselves, it is not sufficient for algorithm performance testing. Also, simplified models do not capture the potentially complex interactional aerodynamic effects that gusts can have on eVTOL/DEP aircraft having closely spaced lift and propulsion rotors. Thus, more detailed models of eVTOL/DEP aircraft for several base configuration types are being studied to assess their gust response sensitivity and thereby develop appropriate dynamic models for use within the estimation algorithm. Two sources of models are presently being studied for assessment of this dual estimation approach: a "stitched" locally linearized flight dynamics model produced from the NASA Design and Analysis of RotorCraft / flight dynamics computation of ordinary differential equations (NDARC / FlightCODE) software combination, and a fully nonlinear model incorporating CDI's Comprehensive Hierarchical Aeromechanics Rotorcraft Model (CHARM) module software in its CHARM toolbox for MATLAB.

NASA has created representative eVTOL/DEP vehicle models using its NDARC (for NASA Design and Analysis of RotorCraft) software (Johnson, Silva, & Solis, 2018), and these vehicle definitions are being used as inputs to the recently developed FlightCODE analysis tool for creation of locally linearized dynamic flight models of these aircraft (McKillip & Keller, 2021). FlightCODE generates extended stability derivative models of aircraft that have been sized within NDARC that represent small perturbation dynamic models at specified trim points identified within the NDARC input data. The linearized aerodynamic models are indexed with flight condition and vehicle configuration parameters and combined with trim control and body forces to couple with a nonlinear kinematic model that can create a continuous flight dynamics model using a "stitching" process described in Tobias & Tischler (2016).

The more extensive models developed for this use incorporate features of the CHARM Toolbox for MATLAB, a developmental environment that incorporates the CDI CHARM Module Wake/Panel model within a MATLAB-based component formulation of an aircraft model for fully nonlinear simulation of vehicle response to both control inputs and external disturbances (McKillip, Keller, Wachspress, Whitehouse, & Quackenbush, 2010). The CHARM Module, which provides rapid vortex-based wake modeling for a wide assortment of flight vehicles, has been extensively correlated with wind tunnel and flight test data, and most recently is used within a fully nonlinear flight simulation tool for eVTOL/DEP aircraft called DEPSim (Theron, Horn, & Wachspress, 2020).

## 4.1   FlightCODE models

Two flight dynamic models of the NASA single-place quadcopter, described in Johnson, Silva, & Solis, (2018), were created using the FlightCODE tool for a hover condition, as takeoff and landing conditions in turbulence are likely to be defining metrics in control power requirements. The first was a simple quasi-static model with no rotor dynamics, and the second included first-order flapping along with dynamic inflow states for all four rotors. A normally distributed random vertical gust was imposed on each model to assess the difference in response between the two representations, as a way of assessing the difficulties in use of the quasistatic model to represent gust response behavior when additional dynamics are present.

Despite the difference in stability derivatives between the two models, their gust response to the imposed random vertical turbulence is almost identical, as seen in Figure 3. This is clearly due to the similarity in the frequency response of the two models over the low-frequency range, seen in Figure 4, where the vehicle is dominated by a heave damping response. This preliminary result suggests that, at this level of modeling fidelity, a low-order approximate model for vehicle

response may be sufficient for estimating low to moderate frequency gust magnitudes. Work with this locally linearized model continues and is being expanded for inclusion of other control mappings for vehicle angular rate responses. This intermediate fidelity model serves a useful role in assisting the understanding of the appropriate level of modeling detail needed to estimate the statistics of the equivalent control required for disturbance mitigation with confidence.
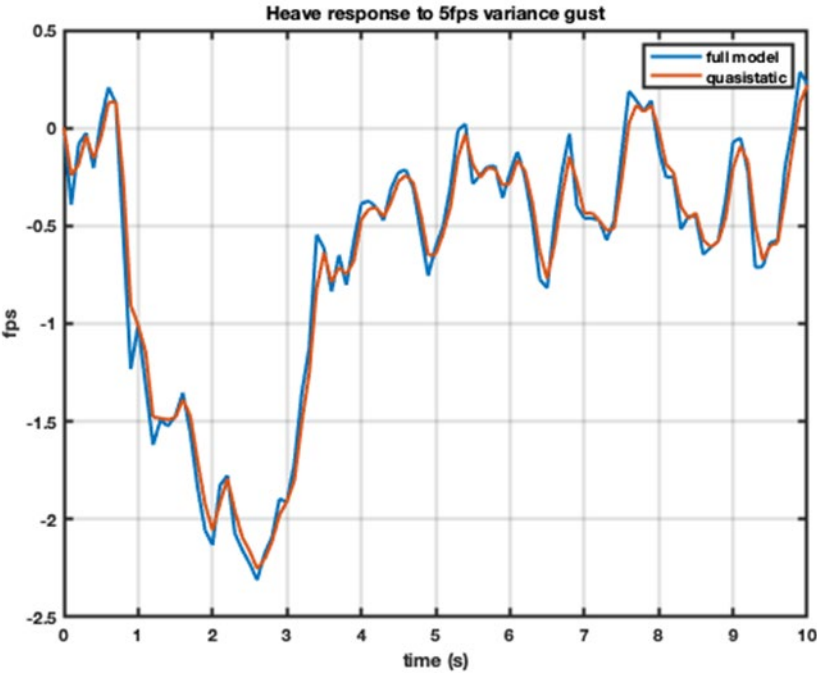


Figure 3. Heave response velocity to vertical gust for different concept quadcopter model DOFs
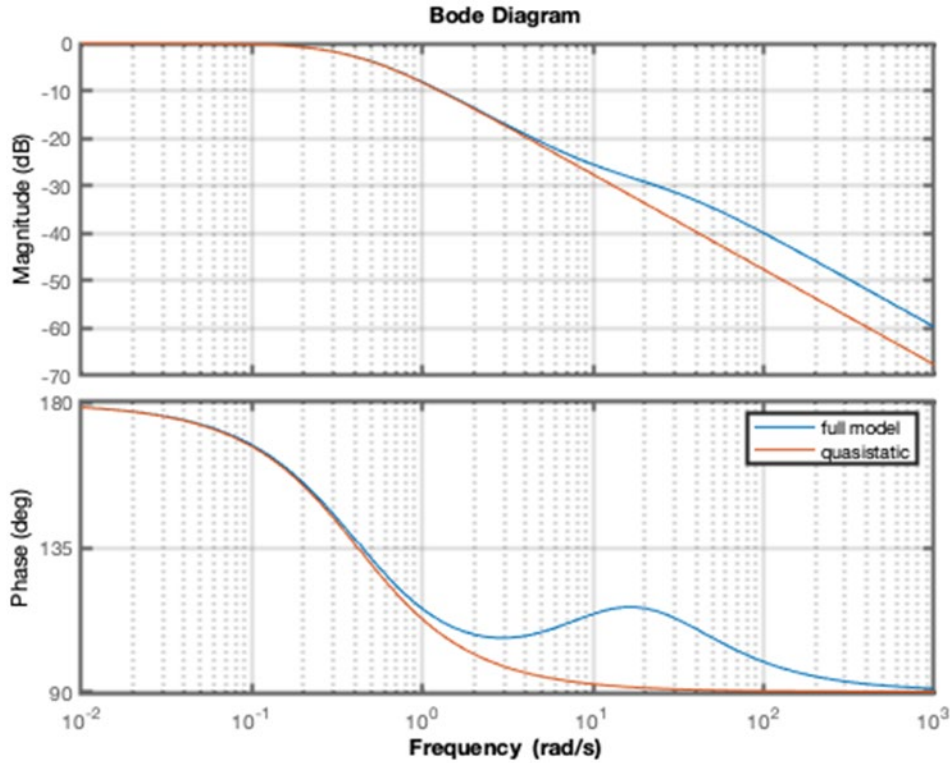
Figure 4. Vertical gust to heave velocity transfer function for different concept quadcopter model DOFs

## 4.2 CHARM Toolbox models

Parameters from the same NDARC reference model used in the FlightCODE model generation were used to create a nonlinear CHARM Toolbox model in MATLAB of the quadrotor single-place concept vehicle. This model includes a full-span wake model coupled to a blade element rotor model, currently only using rigid flap response for the blade dynamics representation. Gust modeling currently only includes uniform variation of the local flow field, thereby impacting local flows and wake filaments similarly, but extensions are being added to permit spatial gust field variations, as are typically seen in operations near bluff bodies (e.g., ship superstructures or urban vertiports). A representation of the wake structure for this aircraft in a 40kt trimmed flight condition can be seen in Figure 5, where the interaction of the aft rotor wakes with the forward rotor wakes is evident, despite the vertical separation of the two lift systems.

The current model is being extended to include mechanical time constants for supporting control designs that modulate thrust on rotor/propellers via rpm variations. Use of rpm control instead of collective pitch control requires accelerating torques to change rotor speeds, and thus generates a transient (dynamic) effect that is compounded with the additional change in the wake

characteristics with thrust changes. To appreciate the time lags associated with wake dynamics effects, a simulation of a 10% increase in rpm for an isolated rotor shows Figure 6an oscillatory transient that settles into a new steady state condition after a quarter second following this step change. This response does not include rotor inertia in the applied torque requirement.
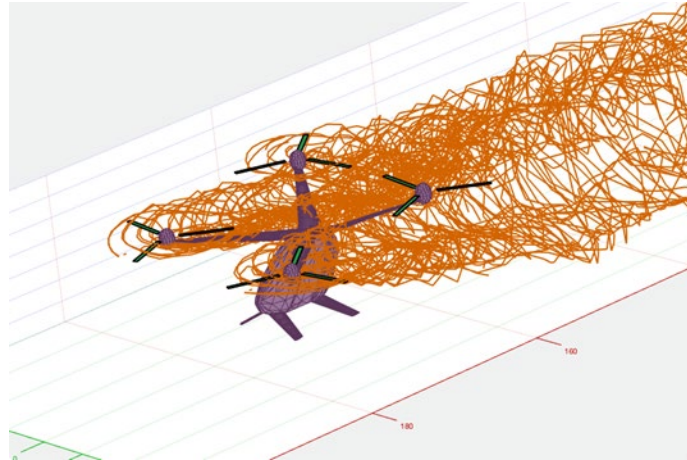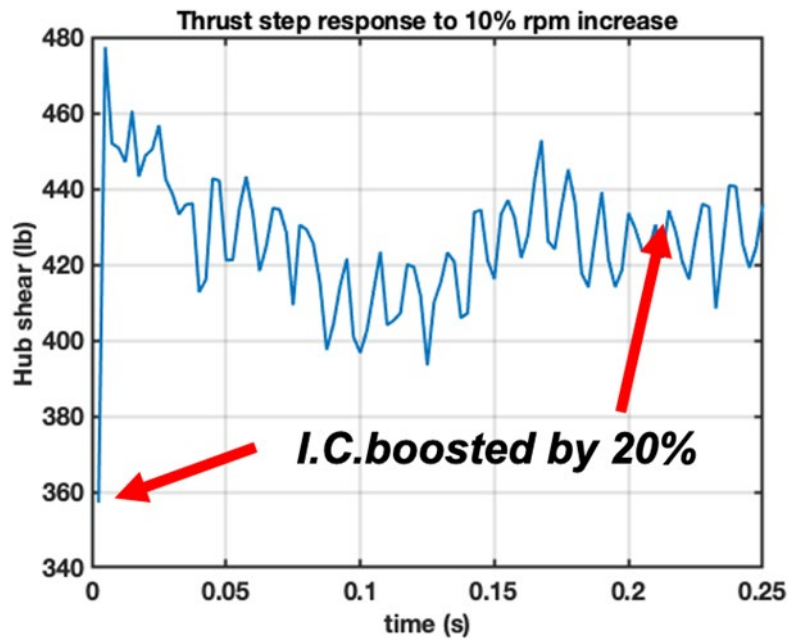


Figure 5. NASA quadcopter wake structure at 40kt cruise



Figure 6. Hub shear transient to 10% step increase in rpm

# 5 Experimental validation

One of the tasks associated with this effort is to explore the implementation issues involved with processing flight data in real time to algorithmically determine remaining control margins and associated gust disturbance magnitudes. This demonstration work is being performed on small UAV platforms that are representative of the types of control configurations present on developmental and planned eVTOL/DEP vehicles. Due to their wide commercial availability and ease of initial integration, the first configuration being investigated is a quadcopter. A Tarot 650 quadcopter has been modified with additional instrumentation and avionics to provide a flying testbed to assess the algorithm's performance in actual turbulent conditions. Figure 7 shows the test model on a strain gauge balance along with one of several 3-axis anemometers being used to collect turbulence measurements in the flight field where testing is taking place. Test instrumentation includes a UAV data board v5 (UDB5) open-source autopilot board that provides both inertial, GPS-derived, and control input and motor output data in a telemetry stream to a data collection and monitoring laptop computer and will ultimately include an on-board processor that implements a form of the above algorithm to determine control equivalent turbulence estimates along with gust state estimates as part of the telemetry frame.



Figure 7. Instrumented Tarot 650 on sting balance with 3-axis anemometry stand

Since the quadcopter is to use a model-based algorithm to extract response residuals between commanded and gust-generated flight data, it is important to properly quantify the model's response to flight (motor) commands. This response can be predicted using the simulation models just described but can also be measured using standard system identification input-output measurements (Tischler & Remple, 2006). In fact, this test article, and others that will follow it,

serve as useful data sources for validation of the simulation tools in predicting control response behavior of these scaled eVTOL/DEP configurations.

Control response testing on the Tarot 650 has been conducted both on a static 6-component sting balance and in-flight trials in calm conditions. Figure 8 shows the measured load transients from a manually generated sweep excitation of a single motor/propeller on the sting-mounted quadcopter, while Figure 9 shows a vertical heave excitation of the same quadcopter while in flight. Sting balance response results provide estimates of elements within the control effectiveness matrix (accelerations due to control inputs), while flight response measurements will include vehicle motion effects (e.g., damping derivatives) for identifying the vehicle system dynamics matrix elements.
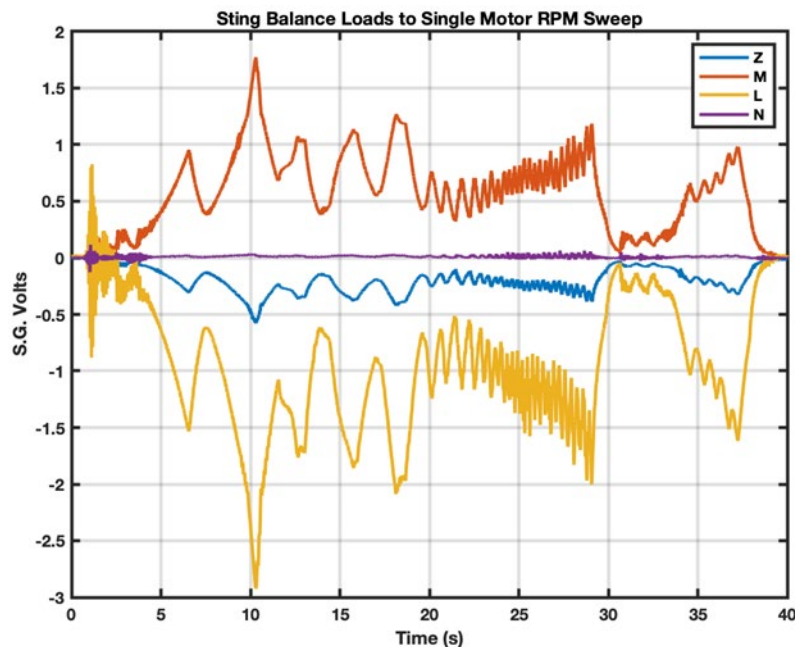


Figure 8. Sting balance time history for single rotor frequency sweep

Instrumentation for this first series of UAV tests required the use of a hybrid style approach, as the recommended core autopilot for the Tarot 650 was used for vehicle stabilization but represents a "black box" in that measured data from its internal IMU/magnetometer/GPS instrumentation is not made available to the operator. Thus, the command signals to the individual motor controllers were routed to the UDB5 board via Y-connectors, and individual optical sensors were installed to collect motor rpm data on each arm. The on-board 6-axis IMU (3 gyros, 3 accelerometers) and a separate patch GPS antenna and integral processor completed the measurement arrangement. A schematic of the installed avionics for this test is shown in Figure 10.
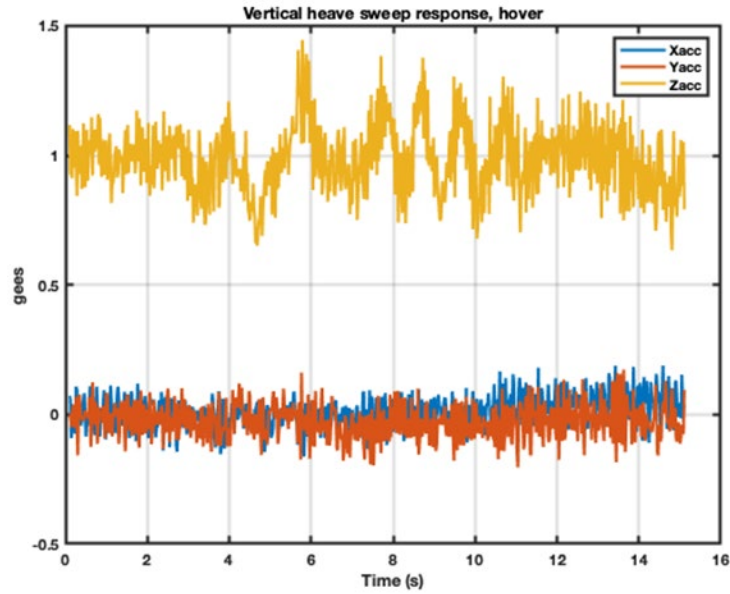
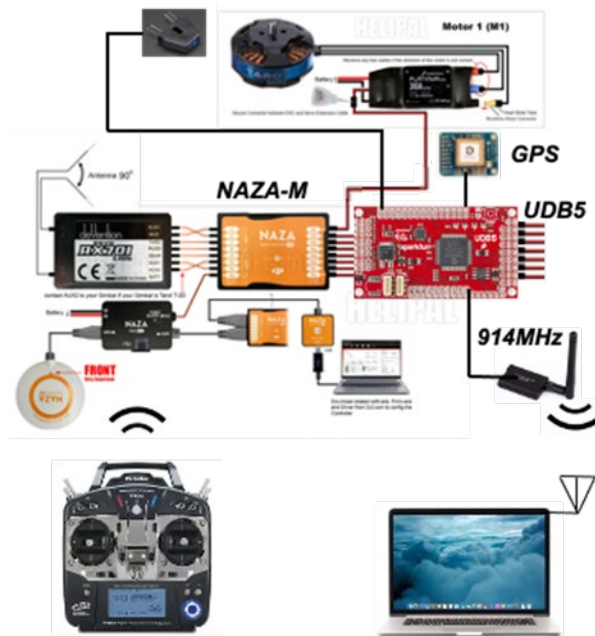Figure 9. Hover heave frequency sweep acceleration response



Figure 10. Tarot 650 quadcopter avionics with added test instrumentation

## 5.1 Disturbance flight testing

Evaluation of the algorithm should ideally determine if the estimated gust disturbance from vehicle response measurements is what is present at the current vehicle location. This implies that the disturbance environment is known, or at a minimum, its statistics (mean and variance) is

quantified over the area of flight operations. Current plans for testing these various representative UAV configurations are to operate them in the exhaust flow area of the FAA's Airflow Induction Test Facility at the Wm. Hughes Tech Center at Atlantic City, NJ. Figure 11 shows the 15-foot radial exhaust port of this blowdown tunnel, which opens onto a concrete pad where the UAV may be flown into and out of the shear flow created by the jet from the operating tunnel.



Figure 11. Exhaust port behind FAA wind tunnel for disturbance flight testing

As this facility was undergoing refurbishment, an alternate venue was used that was also part of the FAA Tech Center facilities at the Atlantic City airport (KACY). A B-737 aircraft with functional engines is located near an access road north of KACY, as seen in Figure 12, and exhausts into a flat triangular field having low brush and minimal vegetation, and thus was used as a surrogate controlled gust environment for disturbance testing of the quadcopter. Since the maximum forward speed of the Tarot 650 is approximately 45mph, the starboard engine was operated at idle thrust throughout the testing activity. Two tests on separate days were conducted at this site, with the first a hover condition in the jet flow, and a second with a translation through the shear layer of the jet exhaust.
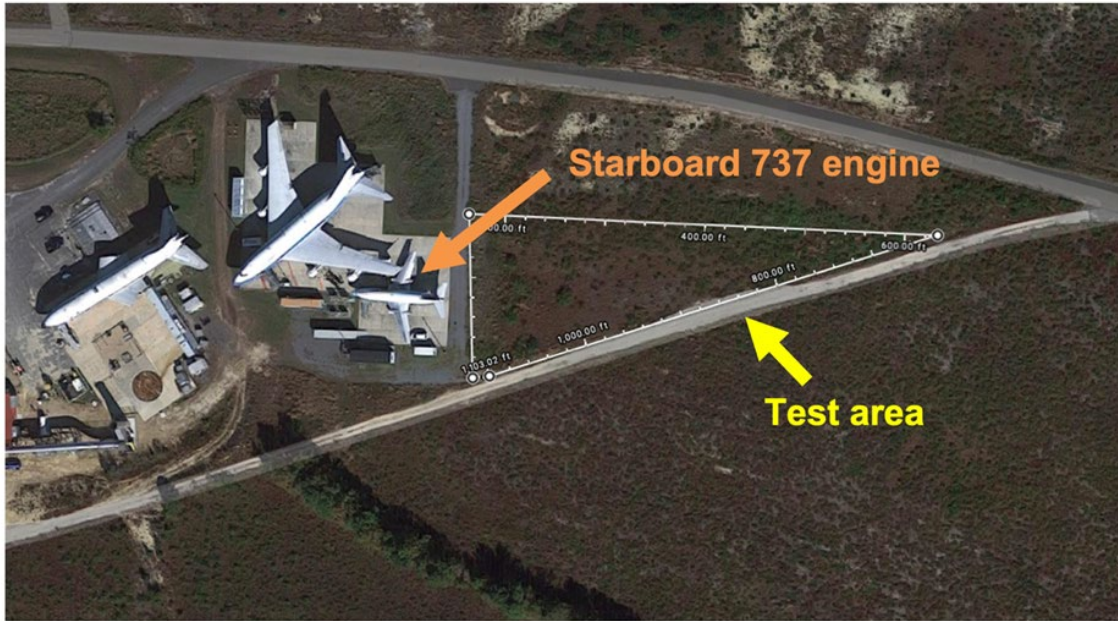
Figure 12. Quadcopter test site (white triangle) behind B-737 engine north of KACY

A 3-axis anemometer was placed at several locations behind the jet flow to collect mean and variance data on the disturbance flow environment. A custom data collection package was used with user real-time display to digitize and store the anemometer data onto a memory card within a Raspberry Pi single board computer, attached to the anemometer array. For the second sortie, the instrumented quadcopter was then flown into and out from the exhaust flow to excite the vehicle response, separate from the pilot controls or autopilot stabilization commands driving the four lift motors. Data was collected throughout the flight trials and monitored on a laptop collecting telemetry over a 940MHz serial data link. Video and still recording of the flight were collected for use in event reconstruction from the telemetry traces. A still image from the flight through the jet exhaust is shown in Figure 13, and the trajectory of the flight paths (on 12/07 in green, and on 12/14 in blue) from the onboard GPS updates is given in Figure 14.

Figure 13. Quadcopter in transition behind B-737 exhaust flow


Figure 14. Quadcopter flight paths for both sorties (hover and transition)

The hover flight tests were conducted at a conservative distance from the B-737 jet exhaust from a location directly in line with the starboard engine. Control of hover was maintained within the disturbance, with stabilizations commands occasionally reaching limits for the associated motor controller. As all flight activity was within the jet exhaust, no definitive change in general character of the measured response and associated remaining control power metric was observed. Thus, the second sortie on 12/14 was planned to have the quadcopter encounter both the jet blast

and ambient wind conditions in a flight across the location of the jet flow, to provide a known change in flow disturbance that would exercise the algorithm's potential for detection of changes in remaining control power.

Figure 15 shows stacked time histories from that transition flight, which started within the jet exhaust flow, transitioning out of the exhaust field, and then returning to (and passing) the initial takeoff location. The plot shows computed values of RCP for the forward (#2) rotor of the quadcopter, along with the GPS velocity, pitch rate, and vertical accelerometer from that flight. The quadcopter experiences the jet blast shortly after liftoff (at 80s), but then transitions further north of the jet flow into relatively benign conditions (at 115s). The high frequency excitation of the quadcopter pitch response while operating in the jet exhaust is evident in the vertical acceleration trace over the approximately 35s operation within the jet flow and reflected in the frequent minimum values in the RCP metric for the motor as the autopilot attempts to mitigate this disturbance. Once the quadcopter is clear of the jet blast, the nominal values of RCP increase above the RCP values while within the jet turbulence, despite the maneuvering flight used to return to the takeoff location. When the quadcopter encounters the jet blast again, at a higher altitude, actual LOC was experienced (near 142s), and the quadcopter pitched forward and sped past the launch location, thus requiring flight termination. These preliminary results show that the simplified algorithm using only control effector limits has a good likelihood of providing useful measurements of remaining control power based on the correlation between this metric and the telemetry and observed vehicle behavior in this test.
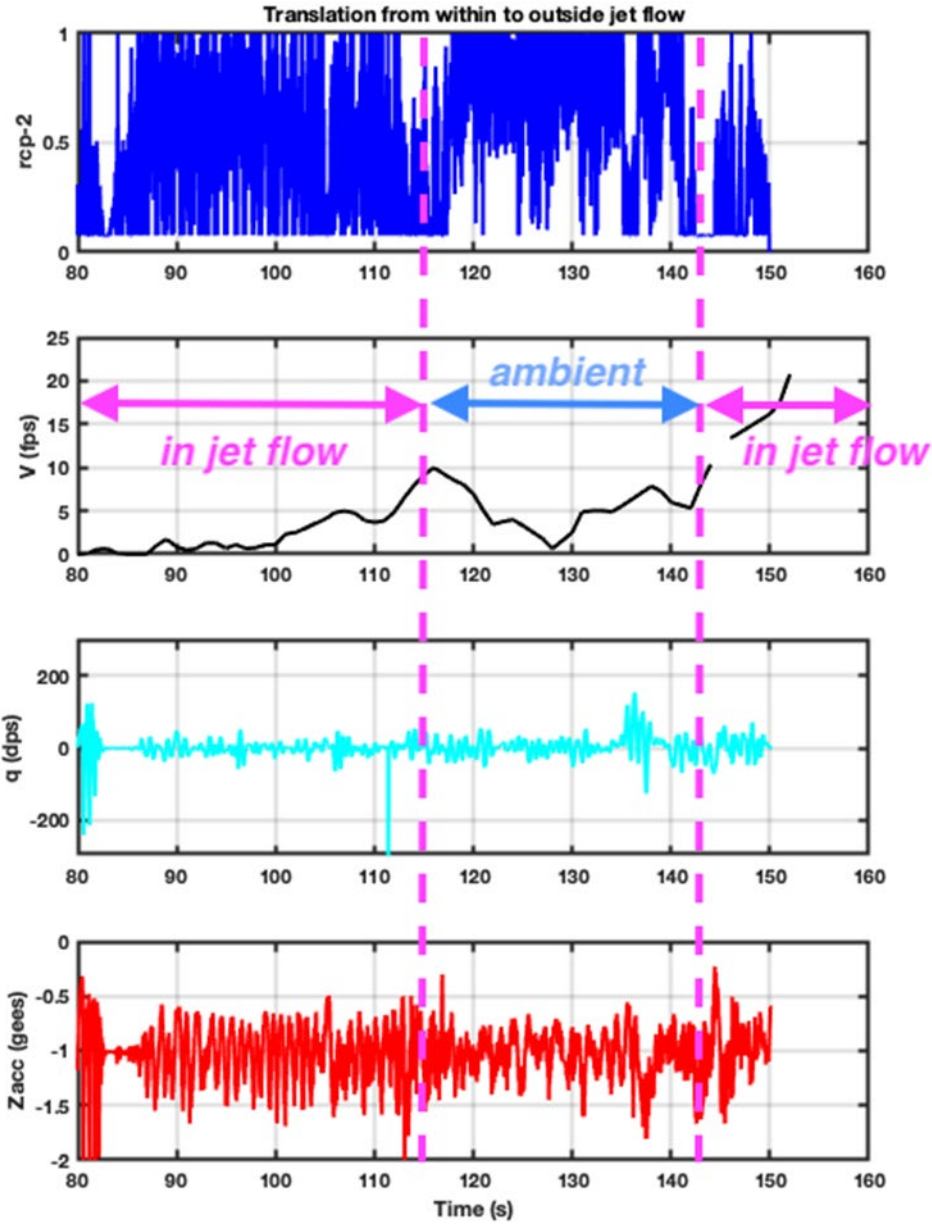
Figure 15. Computed remaining control power RCP with velocity, pitch rate, and vertical accelerometer telemetry during quadcopter transition flight test

# 6 Conclusions

This first year of research has shown that application of algorithms for estimating remaining available vehicle control power, and local gust disturbance magnitudes, appear to provide a usable safety assessment for avoiding loss of control (LOC) events for eVTOL/DEP aircraft. Such real-time safety metrics may aid the challenge of providing safety assurance in certification of these aircraft for operations within the national airspace system. Further testing is being

performed using an integral autopilot and real-time processing engine installed on a backup quadcopter, with plans for using this same system on a Lift+Cruise configuration UAV. Additional work is expanding the algorithm application for control equivalent gust estimation and extraction of local disturbance flows.

# 7    References

American Psychological Association. (2009). *Publication manual of the American Psychological Association.* Washington, D.C.: American Psychological Association.

Chandrasekaran, R., Payan,, A., Collins,, K., & Mavris, D. (2019). *A Survey of Wire Strike Prevention and Protection Technologies for Helicopters.* Technical Report, U.S. Department of Transportation, Federal Aviation Administration. Retrieved from http://actlibrary.tc.faa.gov

Johnson, W., Silva, C., & Solis, E. (2018). Concept Vehicles for VTOL Air Taxi Operations. *Aeromechanics Design for Transformative Vertical Flight.* San Francisco, CA: AHS.

Kochhar, S., & Friedell, M. (1990). User control in cooperative computer-aided design. *UIST '90: Proceedings of the 3rd annual ACM SIGGRAPH symposium on user interface software and technology* (pp. 143-151). ACM. doi:https://doi.org/110.11445/97924.9794

List, A., & Hansman, R. J. (2019). *Assessing Multi-rotor UAV Controllability in Low Altitude Fine-Scale Wind Fields.* Cambridge, MA: M.I.T. International Center for Air Transportation.

Lusardi, J., Blanken, C., & Tischler, M. (2003). Piloted Evaluation of a UH-60 Mixer Equivalent Turbulence Simulation Model. *59th AHS Annual Forum.* Phoenix, AZ.

McConville, A., Richardson, R., & Moradi, P. (2022). Comparison of Multirotor Wind Estimation Techniques Through Conventional On-board Sensors. *AIAA SciTech Forum.* San Diego, CA.

McKillip, J. R., & Keller, J. (2021). *Development of a Rotorcraft Flight Dynamics and Control Modeling and Analysis Tool for Conceptual Design: FlightCODE Theory Manual.* Ewing, NJ: CDI Technical Note 2108.

McKillip, J. R., Keller, J., & Kaufman, A. (2002). Algorithmic Icing Detection for the V-22 Osprey. *Flight Controls and Crew System Design Specialists Meeting.* Philadelphia, PA: AHS.

McKillip, J. R., Keller, J., Wachspress, D., Whitehouse, G., & Quackenbush, T. (2010). Simulation of Dynamic Interface Flight Control Concepts Using the CHARM Toolbox for MATLAB. *Specialists Conf. on Aeromechanics.* San Francisco, CA: AHS.

McKillip, Jr., R. (2018). *Real-time Turbulence Recognition and Reporting System for Unmanned Systems.* Ewing, NJ: CDI Report 18-10, for Navy SBIR Contract N68335-18-C-0348.

McKillip, R. J., & Perri, T. (1992). Helicopter Flight Control System Design and Evaluation Using Controller Inversion Techniques. *Journal of the AHS, 37(1)*, 66-74.

Scruton, R. (n.d.). The eclipse of listening. *The New Criterion, 15*(3), 5-13.

Seher-Weiss, S., & von Gruenhagen, W. (2009). Development of EC 135 Turbulence Models via System Identification. *35th European Rotorcraft Forum.* Hamburg, Germany.

Strunk, W., & White, E. B. (1979). *The Elements of Style* (Third ed.). New York, New York, USA: Macmillan Publishing Co., Inc.

Theron, J., Horn, J., & Wachspress, D. (2020). An Integrated Simulation Tool for eVTOL Aeromechanics and Flight Control. *Aeromechanics for Advanced Vertical Flight Technical Meeting.* San Jose, CA: VFS.

Tischler, M., & Remple, R. (2006). *Aircraft and Rotorcraft System Identification, 2nd Ed.* Reston, VA: AIAA.

Tobias, E., & Tischler, M. (2016). *A Model Stitching Architecture for Continuous Full Flight-Envelope Simulation of Fixed-Wing Aircraft and Rotorcraft from Discrete-Point Linear Models.* U.S. Army RDECOM Special Report RDMR-AF-16-01.

Withrow-Maser, S., Malpica, C., & Nagami, K. (2020). Multirotor Configuration Trades Informed by Handling Qualities for Urban Air Mobility Application. *VFS 76th Annual Forum.* Virtual: Vertical Flight Society.